# A Microjet Array Cooling System for Thermal Management of High-Brightness LEDs

Xiaobing Luo and Sheng Liu

***Abstract*—In this paper, a microjet-based cooling system is proposed for the thermal management of high-power light-emitting diodes (LEDs). Preliminary experimental investigation and numerical simulation on such an active cooling system are conducted. In the experiment investigation, thermocouples are packaged with LED chips to measure the temperature and evaluate the cooling performance of the proposed system. The experimental results demonstrate that the microjet-based cooling system works well. For a 2 × 2 LED chip array, when the input power is 5.6 W and the environment temperature is 28 °C, without any active cooling techniques, the temperature of 2 × 2 LED chip array substrate reaches 72 °C within 2 min and will continue to increase sharply. However, by using the proposed cooling system, when the flow rate of micropump is 9.7 mL/s, the maximum LED substrate temperature measured by the thermocouples will remain stable at about 36.7 °C. As for the numerical optimization, the comparison between the simulation and experimental results is presented to confirm the feasibility of the simulation model. By using the simulation model, the effects of microjet diameter, top cavity height, micropump flow rate, and jet device material on system performance are numerically studied. According to the preliminary test and numerical optimization, an optimized microjet cooling system is fabricated and applied in thermal management of a 220-W LED lamp. The temperature test demonstrates that the cooling system has good performance.**

***Index Terms*—High-brightness light-emitting diodes (LEDs), microjet arrays, numerical optimization, thermal management.**

## I. Introduction

LIGHT-EMITTING diodes (LEDs) have received much attention in recent years because of their advantages compared with common light sources. Currently, the most common light sources are incandescent filament lamp and fluorescent lamp, both of them are associated with large energy losses that are essentially inherent because of high temperatures and large stokes shifts involved [1]. LED depends on semiconductor material to emit the light. Theoretically, it has many distinctive advantages such as high efficiency, good reliability, long life, variable color, and low-power consumption. Recently, LED begins to play an important role in many applications [2]. Typical applications include back lighting for cell phones and LCD displays, interior and exterior automotive lighting including headlights, large signs and displays, signals and illumination.

For modern LEDs, especially for high-brightness LEDs, both optical extraction and thermal management are critical factors for the high performance of LED packaging. Generally, most of the electronic power of LEDs will be converted into heat and this heat will greatly reduce device luminosity. In addition, the high junction temperature will shift the peak wavelength of the LED, which will change the color of the light. Narendran and Gu [3] have experimentally demonstrated that the life of LEDs decreases with increasing junction temperature in an exponential manner. Therefore, low-operation temperature is essential for LEDs. Since the market demands that LEDs have high power and packaging density, it poses a contradiction between power density and operation temperature, especially when applications require LEDs to operate at full power to obtain desired brightness.

To address the thermal problem of LEDs, Arik and Weaver [4] carried out a numerical study to understand the chip temperature profile due to the bump defects. Finite element techniques were utilized to evaluate the effects of localized hot spots at the chip active layer. Sano *et al.* [5] introduced an ultra-bright LED module with excellent heat dissipation characteristics. The module consisted of an aluminum substrate circuit board having outstanding thermal conductivity and workability, with the mount for LED chips being formed into fine cavities with high reflectance to improve light recovery efficiency. Furthermore, the condenser of this LED module was filled with high-refraction resin on the basis of optical simulation. An improvement in luminance of 25% or more was observed by taking the aforementioned measures in their paper. Petroski [6] developed a LED-based spot module heat sink in a free convective cooling system. Cylindrical tube longitudinal fin (CTLF) heat sink was used to solve the orientation problem of LED. Chen *et al.* [7] presented a silicon-based thermoelectric (TE) for cooling of high-power LED. The test results showed that their TE device could effectively reduce the thermal resistance of the high-power LED. Hsu *et al.* [8] reported a metallic bonding method for LED packaging to provide good thermal dissipation and ohmic contact. Zhang *et al.* [9] used multiwalled carbon nanotube and carbon black to improve the thermal performance of thermal interface materials (TIM) in high-brightness LED packaging. Tests showed that such a TIM could effectively decrease the thermal resistance. Acikalin *et al.* [10] used piezoelectric fans to cool LEDs. Their results showed that the fans could reduce the heat source temperature by as much as 37.4°C.

Manuscript received December 10, 2005; revised August 22, 2006. This work was supported by Key Technology Research and Development Program of Hubei Province, China (2006AA103A04).

X. Luo is with School of Energy and Power Engineering and the Wuhan National Laboratory of Optoelectronics, Huazhong University of Science and Technology, Wuhan 430074, China.

S. Liu is with Wuhan National Laboratory of Optoelectronics, and Institute of Microsystems, Huazhong University of Science and Technology, Wuhan 430074, China (e-mail: shengliu63@yahoo.com).

Color versions of one or more of the figures in this paper are available online at http://ieeexplore.ieee.org.

Digital Object Identifier 10.1109/TADVP.2007.898522

1521-3323/$25.00 © 2007 IEEE

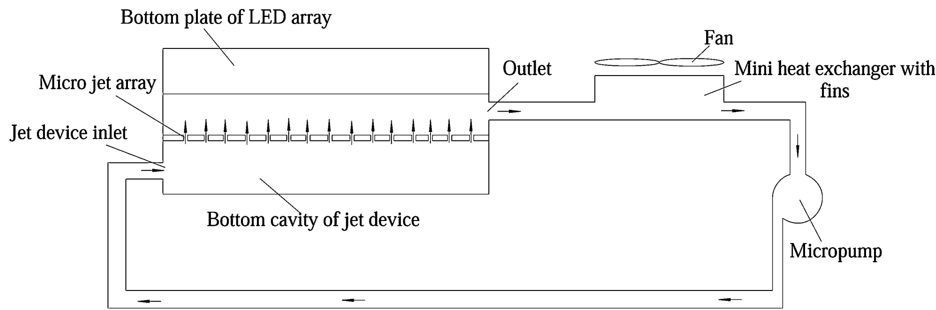


Fig. 1. Present closed-loop microjet array cooling system.

The piezoelectric fans have been shown to be a viable solution for the thermal management of electronic components and LEDs.

Recently, Liu's group began to compare different cooling technologies including a primitive prototype of the microjet array [11]. The results demonstrated the advantages of the microject array as compared to the heat pipe and regular fin-based cooling techniques. In those experiments, the temperature was measured by the infrared thermometer, therefore, only LED surface temperature was obtained, which was far from the junction temperature of LED chips.

In this paper, an enhanced version of the closed microjet array cooling system is proposed to realize the thermal management for high-power density LEDs, in particular for LED array. A small heat exchanger is used for the heat transfer between the system and the environment. Experimental investigation and numerical simulation on such a system are conducted. For achieving relatively exact temperature distribution in LEDs, thermocouples are packaged into LEDs and used for the temperature measurement and cooling effect evaluation. The experiments demonstrate that the present system has good cooling ability; however, the microjet device in the experiment needs to be further optimized. In optimization simulation, the effect of several factors such as microjet diameter, top cavity height, micropump flow rate, and jet device material on the system performance are numerically studied. Based on the preliminary experiment and numerical optimization, a new microjet device is fabricated and applied in a 220-W white light LED lamp.

## II. Microjet Array Cooling System

Fig. 1 demonstrates the closed-loop LED cooling system. It composes of three parts: a microjet array device, a micropump, and a small heat exchanger with a fan. When LEDs need to be cooled, the system starts to work. Water or other fluids or gases in the closed system is driven into the microjet array device through an inlet by a micropump. Many microjets form inside the jet device, which are directly impinged onto the bottom plate of LED array. Since impinging jet has a very large heat transfer coefficient, the heat created by LEDs is easily removed by the recycling fluid in the system. The fluid is heated and its temperature increases after flowing out the jet device, then the heated fluid enters into the heat exchanger with fins and fan. The heat exchanger will cool the fluid and the heat will be dissipated into the external environment. The cooled fluid will be delivered into the jet device to cool the LED array again by the force of the micropump in the system. The above processes constitute one operation cycle of the total system. It should be noted here that the real size of the system can be designed as one small package according to application requirements.

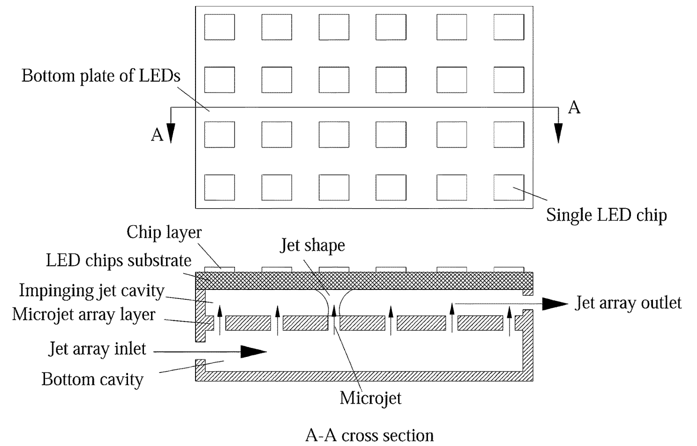


Fig. 2. Microjet array device.

Fig. 2 shows the structure of the jet device of Fig. 1 in detail. It consists of several layers, which are (from the top to the bottom) the chip array layer, the top plate of jet cavity, the impinging jet cavity, the microjet array layer, and the bottom cavity. Cooled fluid enters the device through the inlet, which is opened at one side of the bottom cavity layer. The fluid flows through the microjet array and forms many microjets, as shown in Fig. 2. With enough driving force, the jets will directly impinge onto the chip substrate of LEDs. The heat conducted down through the LED chips will be dissipated into the cooled fluid quickly due to the high heat transfer efficiency of impinging jets. The fluid temperature increases and the heated fluid flows out from the jet array outlet that is opened at one side of the top jet cavity layer. Through such a process, the heat from LED chips will be transferred into the fluid efficiently.

Impinging jet has been demonstrated as an efficacious cooling solution in many applications [12], [13]. To the authors' knowledge, there are no other reports on the use of impinging jet system for cooling LEDs. However, the heat transfer of the microjet device in the proposed system is essentially based on the concept of impinging jet, which has been studied by many other researchers by numerical and experimental

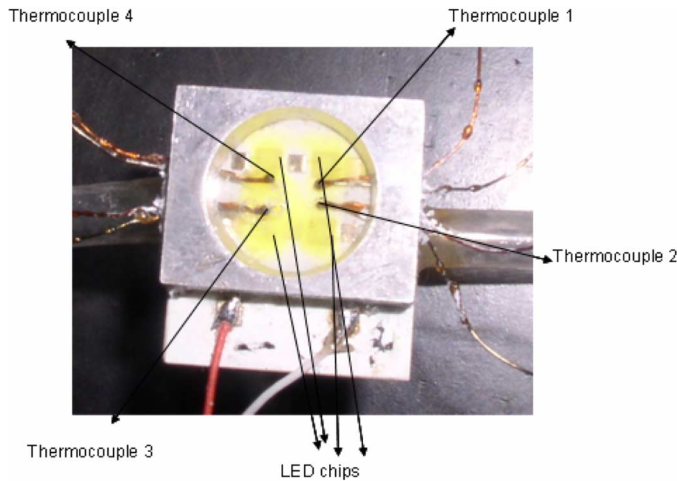


Fig. 3. Tested LED array packaged with thermocouples.

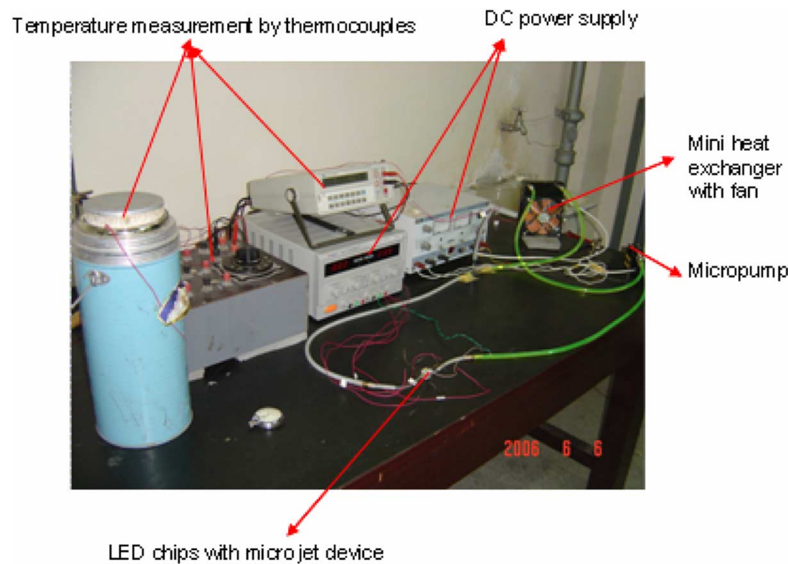


Fig. 4. Experimental setup.

methods. Chattopadhyay [14] performed numerical investigations to predict heat transfer characteristics of laminar annular jets impinging on a surface. It was found that heat transfer from the annular jet was about 20% less compared to the circular jet. Thielen *et al.* [15] investigated the effect of nozzle arrangement on the heat transfer of multiple impinging jets. Two different geometrical arrangements with an equal number of nozzles were studied. It was found that in the circular setup, the individual jets had a similar heat transfer, except for the central jet which was stabilized by the outer jets. In the square setup, the difference between the jets was much more pronounced. Lee *et al.* [16] investigated the effects of nozzle diameter on heat transfer and fluid flow in a round turbulent jet impinging on a flat plate surface. The results showed that the local Nusselt numbers increased with the increasing nozzle diameter in the stagnation point region corresponding to $0 < \mathrm{r/d} < 0.5$. The effect of the nozzle diameter on the local Nusselt numbers was negligibly small at the wall jet region corresponding to $\mathrm{r/d} < 0.5$. Ramezanpour *et al.* [17] numerically studied the heat transfer rate in the turbulent, unconfined, and submerged impinging jet by using a commercial finite volume code called FLUENT. The numerical results predicted the heat transfer rate in flat plate impinging jets by less than 10% difference in comparison with experiments, for inclined impinging jets in different HD, the prediction showed 5%–20% difference.

The present system is different from many normal impinging jets in that they are close-looped in one device. The jets converge into one flow and go out from one outlet, the flow and heat transfer for different jets interact with each other. From this viewpoint, the heat transfer and flow characteristics of the present microjet device are different from those of existing jets.

## III. Temperature Measurement and Experimental Setup

### A. Temperature Measurement and LED Chip Array

Fig. 3 shows one $2 \times 2$ LED package that is packaged with four thermocouples embedded inside the module. It is difficult to test LED junction temperature directly by thermocouples. Present experiment is to check the cooling ability of the proposed concept, the exact measurement of the LED junction temperature is not the target of this paper. Four thermocouples are packaged into our LED device; they are located inside the packaging resin and very close to the LED chips. According to this LED packaging configuration, it is possible that the temperatures achieved by these thermocouples can indicate the order of magnitude of LED junction temperature. In the latter section of this paper, the comparison between experiment and simulation proves this viewpoint.

Fig. 3 also demonstrates the chip distribution of the $2 \times 2$ LED chip array used in the experiment. The four LED chips are distributed on a substrate. Every two chips are connected in series, and then they have been connected in parallel with each other. The size of each LED chip is 1 mm $\times$ 1 mm. The substrate size is 15 mm $\times$ 15 mm.

### B. Experimental Setup

Experimental system is constructed as shown in Fig. 4, which is nearly the same as the one shown in Fig. 1. The micropump in the experiment is based on electromagnetic principle, which is custom designed and made locally in China. Its maximum power consumption is about 2.16 W. The mini heat exchanger and fan is bought from commercial electronics market, and its default power consumption is about 3.6 W. Since the heat transfer efficiency of the microjet device is our experimental focus, the sizes of mini heat exchanger and micropump are relatively large, which can be seen in Fig. 4. In actual applications, it may be reduced for volume and power saving. The working media of the system is distillated water, the flow rate of the micropump is adjustable with the input power, and at default input power is 9.7 mL/s. For the microjet device in the experiment, there are 16 microjets distributed inside, the diameter of each jet is 0.5 mm.

### C. Accuracy Analysis

In the experiments, temperature is the main parameter for system evaluation, and it is directly measured by thermocouples. Since there are no other indirectly measured parameters,

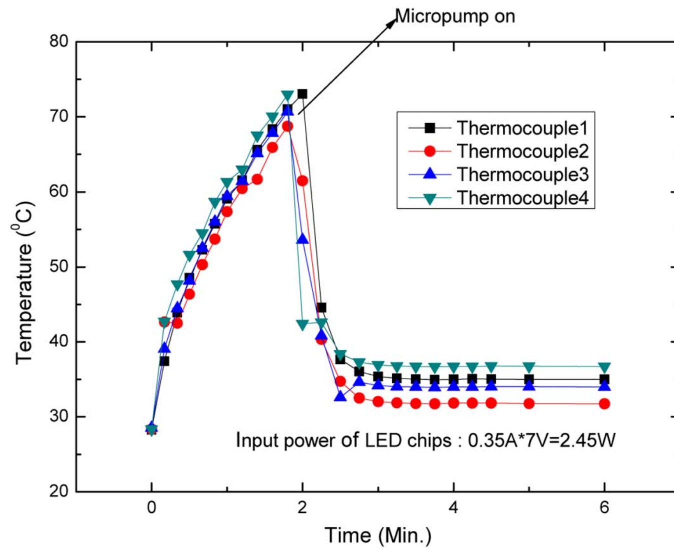

Fig. 5. LED temperature variation with time when pump is off and on.

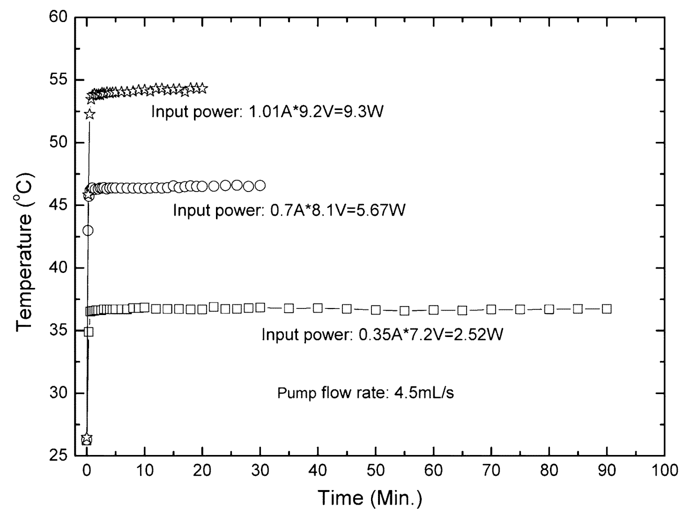

Fig. 6. LED temperature variation with time at different LED input powers.

the errors appeared in this experiment mainly include the measurement error of thermocouples and the reading error of digital multimeter.

The standard T type thermocouples (Cu–CuNi) are used. The cold junction of the thermocouples is an ice and water mixture at 0 °C. To avoid that the mineral impurities in water change its freezing point, the ice is made from the distilled water. The ice bath is put into a vacuum flask to maintain constant temperature for a long time. Therefore, the error produced in the cold junction reference is negligible. For the thermocouples, at the temperature range from −30 °C to 150 °C, the measurement error will be about 0.2 °C. The digital multimeter is HP 3468A, its identification error is about 0.01 °C. Therefore, the total error of the temperature measurement is about 0.21 °C.

## IV. Experimental Results and Analysis

Fig. 5 shows the variation of LED temperatures with time. Here, the total input power of four LED chips is 2.45 W, the flow rate of the micropump is 9.7 mL/s. In this case of experiment, initially, micropump does not work. After LEDs light up for about 2 min, micropump begins to run. It can be seen from Fig. 5 that the LED temperature measured by the thermocouple 4 is the largest in four thermocouples. When the cooling system does not work, LED temperature increases very quickly, within 2 min, the temperature measured by thermocouple 4 increases from 28 °C to nearly 72 °C and it will continue to increase sharply. However, when the micropump begins to operate, the cooling system starts to operate, the temperature measured by thermocouple 4 decreases from 72 °C to 36.7 °C within 1 min. The comparison clearly demonstrates the cooling performance of the proposed system. From Fig. 5, it is found that the LEDs reach steady temperature situation very rapidly with the condition that heat exchanger can dissipate the heat into the environment efficaciously. In Fig. 5, it should be noted that the four thermocouples display the different temperatures. The maximum temperature difference appears between thermocouple 4 and thermocouple 2, it is about 5 °C when the LED temperatures reach stable state. It should be noted that for the input current in the two series, some measures are taken to assure that the power dissipation for each chip is nearly same. First, the same chips from CREE Company are selected. Second, when the electrical substrate is fabricated, the electrical resistances in two series keep nearly same. Third, after the four chips are packaged into the electrical substrate, the currents in the two series are measured to assure that they are nearly same. Since the above several measures assure that every chip receives the same input power, the temperature difference of the four thermocouples in Fig. 5 can be attributed to the nonequable cooling effect by microjet device, the temperature uniformity needs to be improved, sizes and distribution of the microjets should be optimized.

Fig. 6 shows the variation of LED temperature with time at different LED input power levels with the same flow rate of micropump. Here, the flow rate of micropump is 4.5 mL/s. The temperature data in both cases are obtained by thermocouple 4. It can be seen that when the input power of LEDs is 2.52 W, the steady state temperature is 36.7 °C. However, when the input power increases to 9.3 W, the LED temperature keeps steady at about 54 °C.

Fig. 7 shows the variation of LED temperature with time at different pump flow rates with the same LED input power. It can be seen that with the pump flow rate increasing, LED temperature decreases. When the flow rate of the micropump is 3.2 mL/s, the temperature measured by the thermocouple 4 is nearly 39 °C, however, when the flow rate increases to 9.7 mL/s, LED temperature will decrease to about 33 °C. It is easy to explain the phenomena. When pump flow rate increases, heat transfer coefficient of impinging jet in the microjet device will increase, thus the heat from LED chips will be taken out more efficaciously. However, it should be notified that with the pump flow rate increasing, the micropump will consume more power, which will increase the operation cost. In real application, there should be some tradeoff in design between the heat transfer efficiency and the power consumption.

Based on Fig. 7, the efficiency of the microjet cooling system can be estimated. The thermal resistance between the microjet and the substrate can be represented as

$$R_{\mathrm{th}} = \eta R_{\mathrm{mj}} + R_{\mathrm{sub}} \tag{1}$$

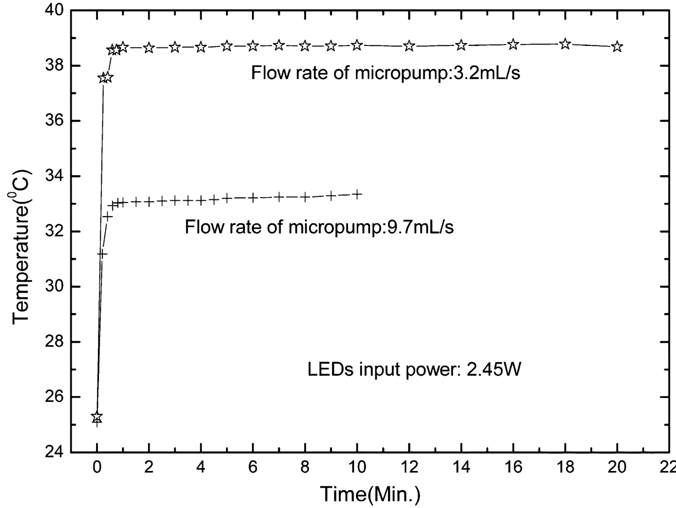


Fig. 7. LED temperature variation with time at different pump flow rates.

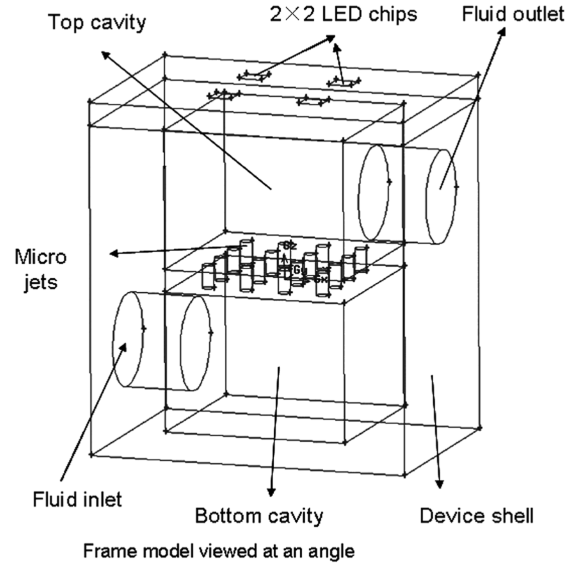


Fig. 8. Simulation model.

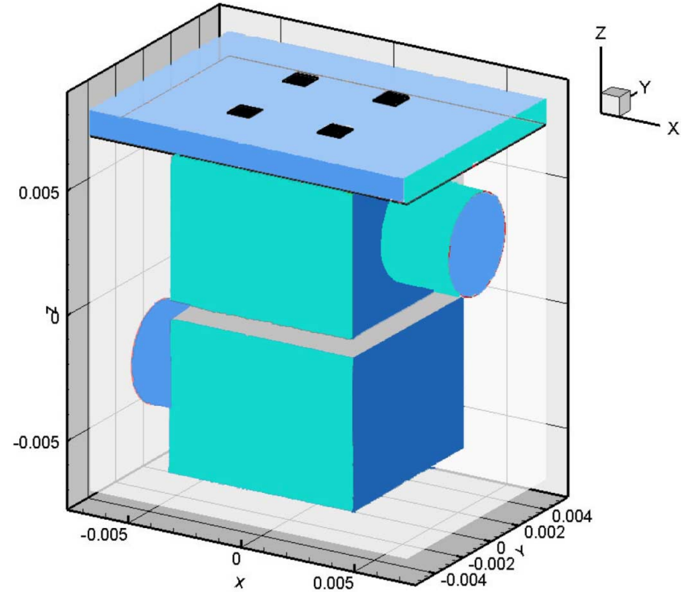


Fig. 9. Three-dimensional structure of present model.

where $\eta$ is a measure for the microjet cooling efficiency, $R_{\rm mj}$ is the thermal resistance of the microjet based on the flow rate, $R_{\rm sub}$ is the thermal resistance of the substrate and $R_{\rm mj}$ can be written as

$$R_{\rm mj} = \frac{1}{\rho \cdot {\rm Fl} \cdot C_p} \tag{2}$$

where Fl is the flow rate and $C_p$ is the heat capacity.

Applying the measurement data and water properties to (1) and (2), it is found that

$$\frac{33 - 28}{2.45} = \eta \frac{1}{9.7 \times 4.18} + R_{\rm sub} \tag{3}$$

$$\frac{38.5 - 28}{2.45} = \eta \frac{1}{3.2 \times 4.18} + R_{\rm sub}. \tag{4}$$

Eliminating $R_{\rm sub}$ from (3) and (4), it is easy to get $\eta = 44.8$.

This means that the thermal resistance of the microjet array cooling system is 44.8 times larger than the theoretical minimum, the efficiency of the microjet device in the present experiments is very low.

It is obvious that the design of microjet device below the LED chips is the key for increasing heat transfer efficiency. For the components in the system, since no intention has been made to optimize the dimensions, materials and structures, the cooling potential of the cooling system does not display, as demonstrated in the above thermal analysis. The low efficiency in the experiments shows that there is much room for improvement. Based on (1), (3), and (4), it is also found that the proposed water cooling system is not advantageous for the low power application. In fact, the present experiments just provide some understanding for the system, the real target for this study is to use the system in super high-power LEDs, as shown in 220-W LED lamp application in the final part of this paper. To prove the above viewpoint, by using the above thermal analysis, it is found that for the microjet device in 220-W LED lamp, the value of $\eta$ is about 1.13, the efficiency of the microjet cooling system in 220-W lamp significantly improves because of the later numerical optimization and high-power application. In addition, with consideration to the cooling cost, the present system is also not suitable for low power situations. In such case, the passive cooling is enough.

Anyway, the numerical optimization is necessary to increase the efficiency and minimize the cost involved as long as our model is reasonably verified.

## V. Numerical Model and Its Validation

The microjet device is the key part of the cooling system. Its cooling performance determines the cooling effect of total system. As shown in Fig. 2, the device is small and the impinging jets are in a closed space, the sensor distribution and measurement are difficult to implement without sophisticated micro sensors, numerical simulation is an effective way to understand and optimize the flow and temperature distribution in the microjet device. Based on the experimental system and microjet device that has been fabricated by us, numerical

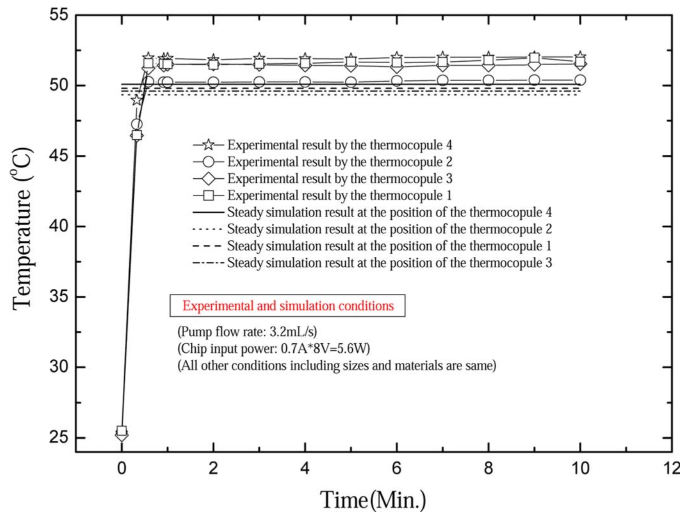


Fig. 10. Temperature comparison between experiments and simulation with small pump flow rate.

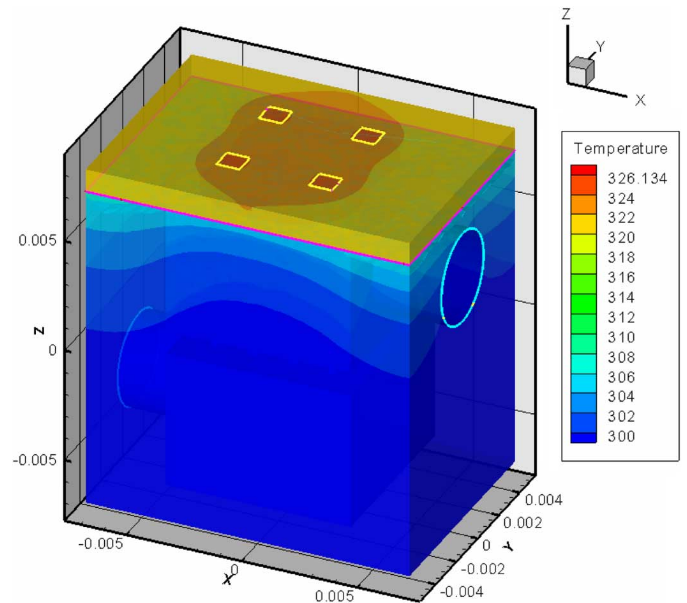


Fig. 11. Temperature distribution of microjet device and chip junction by simulation.

models are built with a typical one shown in Figs. 8 and 9. Fig. 9 demonstrates the three dimensional structure described by Fig. 8. In Fig. 9, the inside structure including the top cavity, bottom cavity and microjets can be seen after the treatment of translucency and lighting.

From Fig. 8, there are several heat transfer means in the microjet device: LED chips produce heat, nearly all the heat will be transferred to impinging jet flow and jet device shell by forced convection and conduction, respectively. For the latter, the heat in the jet device shell will exchange with the environment by natural convection. Such a model reflects a coupled heat transfer process including natural convection, liquid forced convection, and conduction. Here, commercial CFD code Fluent 6.2 is used for simulation.

In Figs. 8 and 9, the size of single LED chip is 1 mm $\times$1 mm. The length, width, and height of microdevice are 14, 10, and 14 mm, respectively. The diameter of the microjet is 0.5 mm; the number of microjets is 16. The diameter of fluid inlet and outlet is 4 mm. The fluid inlet adopts the boundary condition of constant flow rate. The turbulence model in simulation is standard $k-\varepsilon$ model. Convergence study on grids is conducted before the calculation. They are refined until the flow field changes by 0.5%. Finally, 381, 889 grids are used in the simulation. The residual control of the continuity equation is 0.001%.

To verify the feasibility for the above model, the corresponding experiments are conducted. The conditions for both the experiment and simulation are exactly the same.

Fig. 10 shows the temperature comparison between experiments and simulations. Here, the pump flow rate is 3.2 mL/s, the total input power of LEDs is 5.6 W. It can be seen from Fig. 10 that the steady temperatures measured by the four thermocouples are about 51.9 °C, 50.4 °C, 51.4 °C, and 52 °C, respectively. The steady simulation temperatures at the positions of the four thermocouples are about 49.8 °C, 49.4 °C, 49.6 °C, and 50.4 °C, respectively. The temperature difference between the experiment and the simulation are about 2.1 °C, 1 °C, 1.8 °C, and 1.6 °C, the error of the simulation results compared with the experimental one are about 4%, 2%, 3.5%, and 3%. This comparison demonstrates that the simulation model can be used for numerical calculation and optimization.

Fig. 11 shows the simulated temperature distribution of the microjet device, LED chips, and their substrate. In Fig. 11, the maximum simulation temperature is about 53 °C, which appeared in the positions of the four LED chips, such a temperature can reflect the LEDs junction temperature magnitude. It is noted that the maximum temperature achieved by the steady simulation is slightly higher than that by the experiments. It can be explained as follows. The maximum temperatures achieved by the thermocouples do not display the values of the chip junction temperatures. Although the positions of the thermocouples are very close to the LED chips, their measured values are lower than the real chip temperatures because of the thermal resistance between the substrate and the LED chips. Based on the above analysis, it can be concluded that the measured temperature in the experiments can reveal the approximate junction temperature magnitude.

## VI. Numerical Optimization

LED chip temperature and flow resistance of the microjet device are two key indexes for evaluating the cooling performance, the former denotes the cooling performance of the microjet device, and low chip temperature shows that the microjet device has good cooling ability. Flow resistance indicates basic power consumption of the micropump in system. Hopefully, an optimized design should result in a low LED chip temperature and small flow resistance.

For the microjet device, the following several factors such as top cavity height, microjet diameter, pump flow rate, and jet shell material have significant effects on the system performance. Therefore, to understand the effect of the above factors

TABLE I
CHIP TEMPERATURE AND FLOW RESISTANCE WITH DIFFERENT CAVITY HEIGHTS

| Top cavity height(mm) | Maximum temperature of LED chips (℃) | Flow resistance (Pa) |
|---|---|---|
| 6 | 48.36 | 48247.122 |
| 4 | 47.45 | 48450.1 |
| 2 | 46.62 | 36890.877 |

on cooling performance of the system, they will be examined in details in this paper.

## VII. EFFECT OF TOP CAVITY HEIGHT

To investigate the effect of top cavity height on the cooling performance and the flow resistance of the present microjet device, three cases are studied, in which the heights of three cavities are 6, 4, and 2 mm, respectively. In this comparison, all other conditions such as the input power, the inlet velocity and other sizes except top cavity height are the same. In simulation, the input power of single LED chip is 1.2 W, thus the total input power is 4.8 W. The inlet flow rate is 12.5 mL/s. Table I shows the results for the three cases.

Here, as shown in the above analysis, maximum chip temperature can indicate the cooling performance of the microjet device. It can be seen from Table I that as the cavity height decreases, the chip temperature decreases slightly, the flow resistance increases firstly, and then it decreases. In Table I, when the top cavity height is 6 mm, the maximum temperature of LED chips is 48.36 °C, the flow resistance is 48247.122 Pa, as the cavity height decreases to 4 mm, the chip temperature just reduces 0.5 °C, the flow resistance increases a little, it is about 48450.1 Pa. When the cavity height decreases to 2 mm, the chip temperature reduces less than 2 °C compared with that in 6 mm case, the flow resistance decreases to 36890.877 Pa. Fig. 12(a) and (b) shows the flow distributions of the two cases. It is clear from Fig. 12 that for a 6 mm cavity height, the impinging jets do not fully touch the above surface of the top cavity, however, for 2 mm case, this situation improves slightly, and the jets can directly impinge on the top surface. Since the heat source is on the top surface of the cavity, obviously, the jets in 2 mm case will meliorate the cooling effect of the microjet device. However, from Table I, it is surprising that cooling effect does not improve significantly, the chip temperature just decreases less than 2 °C.

From 12, the flow resistance variation in Table I can be explained. There are two factors to affect the flow resistance in microjet device. One is local pressure loss in top cavity, the other one is local pressure loss from the top cavity to the outlet. It is noted that the flow channel in the top cavity for 2 mm case becomes much narrower compared with that in 6 mm case. There are many vortexes in the top cavity for 2 mm case, which will produce local pressure loss. However, for the case with 6 mm cavity height, the shape change from the top cavity to the outlet is much sharper than that for 2 mm cavity height case. It will result in that the flow resistance in 6 mm case greatly increases. Considering the above two factors together, it is easy to understand the flow resistance change in Table I.

The above comparison demonstrates that decreasing cavity height does not have significant effect on raising cooling ability;

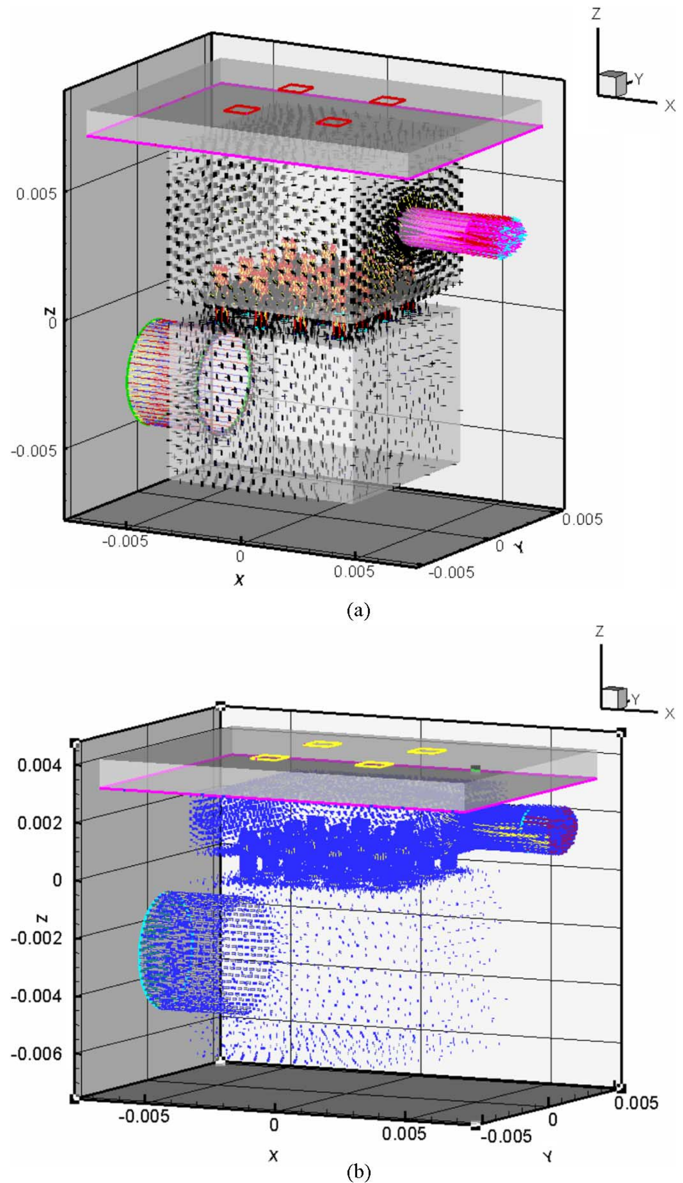


Fig. 12. (a) Flow distribution for 6 mm case. Flow distribution for 2 mm case.

however, to decrease the power consumption of the micropump and system, the cavity height should be optimized.

## VIII. EFFECT OF MICROJET DIAMETER

In order to understand the effect of the microjet diameter on flow resistance and cooling performance, three designs with different microjet diameters are numerically studied. The total input power for the four chips is 4.8 W; the flow rate is 12.5 mL/s. The top cavity height is 2 mm. Table II demonstrates the comparison results. Here, maximum chip temperature is still

TABLE II
CHIP TEMPERATURE AND FLOW RESISTANCE WITH DIFFERENT JET DIAMETER

| Micro jet diameter(mm) | Maximum temperature of LED chips(℃) | Flow resistance (Pa) |
|---|---|---|
| 0.5 | 46.72 | 76071.55 |
| 1 | 34.17 | 63683.47 |
| 1.5 | 47.3 | 55995.4 |

TABLE III
CHIP TEMPERATURE AND FLOW RESISTANCE WITH DIFFERENT PUMP FLOW RATE

| Pump flow rate (mL/s) | Maximum temperature of LED chips(℃) | Flow resistance (Pa) |
|---|---|---|
| 12.5 | 48.63 | 18928.83 |
| 6.25 | 49.4639 | 4973.679 |
| 3.1 | 50.10 | 1368.33 |

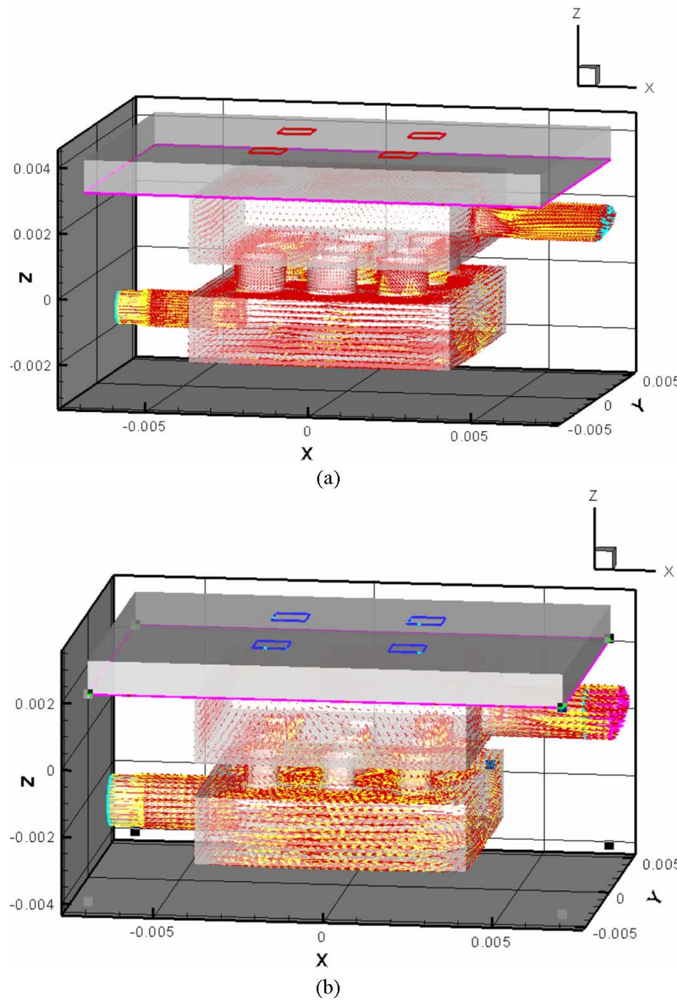


Fig. 13. (a) Flow distribution with 1.5-mm jet diameter. (b) Flow distribution with 1-mm jet diameter.

used as denotation for evaluating the cooling performance of the microjet device.

From Table II, it is found that the microjet diameter has important effect on the cooling performance. For the case of 0.5 mm diameter, the LED temperature is 46.72 °C, as the diameter changes to 1 mm, the temperature sharply decreases to 34.17 °C. However, when the diameter is 1.5 mm, the LED temperature is 47.3 °C. This variation trend demonstrates that for the present simulation conditions, the diameter has an optimized value, which needs further detailed simulation for achieving the exact number. Fig. 13(a) and (b) display the flow field in the microjet device with 1.5 mm and 1 mm micro in jet diameter, respectively. From Fig. 13(b), it can be seen that the impinging jet and flow disturbance in the case of 1-mm jet diameter is much stronger than that in the case demonstrated in Fig. 13(a); this is the main reason for that cooling effect with 1-mm jet diameter is much better than that with 1.5-mm jet diameter.

From Table II, it is also found that as jet diameter increases, the flow resistance reduces. This can be easily understood. With the same flow rate, when the jet diameter increases, the pressure loss will decrease. Thus, the flow resistance will be reduced.

## IX. EFFECT OF MICROPUMP FLOW RATE

As for the effect of pump flow rate, it is expected that with the increase of the pump flow rate, the chip temperature will greatly decrease, the flow resistance sharply increases. Table III demonstrates the effect of pump flow rate on the cooling performance and flow resistance. From Table III, it can be seen that as the flow rate increases, the flow resistance increases sharply, however, the LED chip temperature just decreases a little. These results show that the cooling performance is not so that dependent on the flow rate. Compared with the microjet diameter shown in Table II, the flow rate does not have a significant effect on the cooling performance. The above phenomena are mainly attributed to the small input power of LED chips.

From Table III, it also can be seen that the flow resistance is strongly affected by the pump flow rate, this accords with common sense of fluid dynamics, especially for microjet impinging.

## X. EFFECT OF SHELL MATERIAL OF MICROJET DEVICE

The shell of the microjet device has tight contact with LED substrate; therefore, heat will be conducted from LEDs to the shell of the microjet device. Some of the heat will dissipate to liquid in the microjet device, some of the heat will exchange with the environment by nature convection through the shell surface. The shell material will have effect on the heat conduction process from LED substrate to jet device shell. Table IV demonstrates the effect of shell material on cooling performance and flow resistance of the microjet device.

TABLE IV
CHIP TEMPERATURE AND FLOW RESISTANCE WITH DIFFERENT SHELL MATERIAL

| Shell material | Maximum temperature of LED chips(℃) | Flow resistance (Pa) |
|---|---|---|
| Aluminum | 48.63 | 18928.83 |
| Copper | 45.84 | 18493.31 |

From Table IV, it can be seen that when the shell material is copper, the maximum temperature of LED chips will be lower than that in the case of aluminum shell. Since the thermal conductivity of copper is much larger than that of aluminum, compared with aluminum shell, small parts of the heat produced by LEDs will dissipate to copper shell more efficaciously; the thermal resistance of this process for copper shell is smaller than that of aluminum shell. Therefore, the cooling performance of microjet device made by copper will be better than that of microjet device made by aluminum.

According to Table IV, it is also found that the shell material has little effect on the flow resistance of microjet device. As mentioned above, the shell material affects the heat transfer in total device, thus the temperature distribution of the liquid in the microjet device also changes with the shell material variation, further, the temperature distribution in liquid results in the change of flow distribution and flow resistance. Although the above effect does exist, it is limited. The above description can help understand the data presented in Table IV for the flow resistance variation with the different shell materials.

The above optimization analysis demonstrates that there is much room for improving the design of the microjet device, refabrication and test for the proposed microjet device in the next step is necessary for improving the system performance.

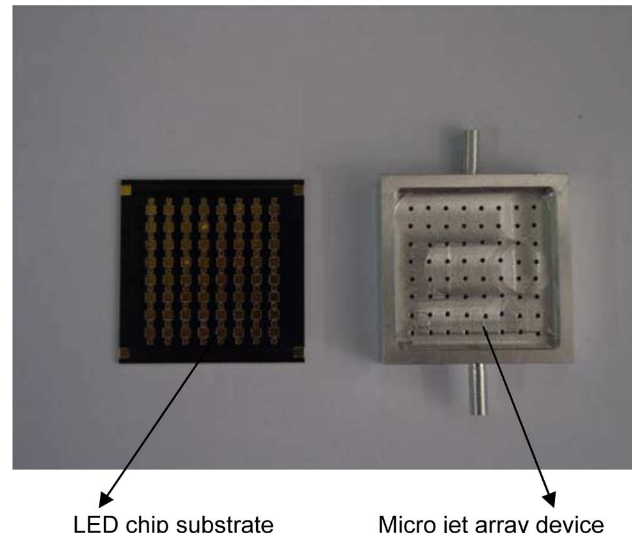


Fig. 14. LED chip substrate and microjet array device.

Fig. 15. Demonstration system of 220-W LED lamp cooled by present system.

## XI. APPLICATION OF THE COOLING SYSTEM IN A 220-W LED WHITE LIGHT SOURCE

A new microjet array is designed and fabricated according to the numerical optimization, which is used for cooling a high-power LED light source. The microjet device and LED chip substrate are shown in Fig. 14. 64 microjets are uniformly distributed in a 3.6 cm $\times$ 3.6 cm cavity. The diameter of the microjet is 1 mm. The default power input about this lamp is about 220 W. For such an application, the power consumption of fan and micropump are about 3.6 W and 2.2 W, respectively. The 220-W LED lamp consists of 64 high-power LED chips which are packaged on a 4 cm $\times$ 4 cm metal substrate. Fig. 15 shows the demonstration system.

Fig. 16 shows the LED substrate temperature variation with the input power of this lamp. It can be seen from Fig. 16 that when the room temperature is 30.8 °C, the temperature of LED chip substrate is about 69.4 °C with 227 W input power of LEDs, which demonstrate that the present cooling system works well.

## XII. SUMMARY

In this paper, an enhanced version of a closed microjet cooling system for LEDs thermal management is proposed. To evaluate its cooling performance, four thermocouples are packaged into the LED chips to measure the LED temperature. The performance experiments demonstrate that the system can have good cooling performance, but the microjet array device needs parameter optimization. The numerical optimization is also conducted in this paper. The effects of top cavity height, microjet diameter, micropump flow rate, and shell material of jet device on the cooling performance and the flow resistance are studied. Numerical optimization results show that microjet diameter has significant effect on cooling performance of the microjet device. As to the present design, an optimized microjet diameter exists for achieving the best flow and heat transfer characteristics. The pump flow rate strongly affects the flow resistance of the microjet device. With the increase of the pump flow rate, the flow resistance sharply increases; however, the cooling performance

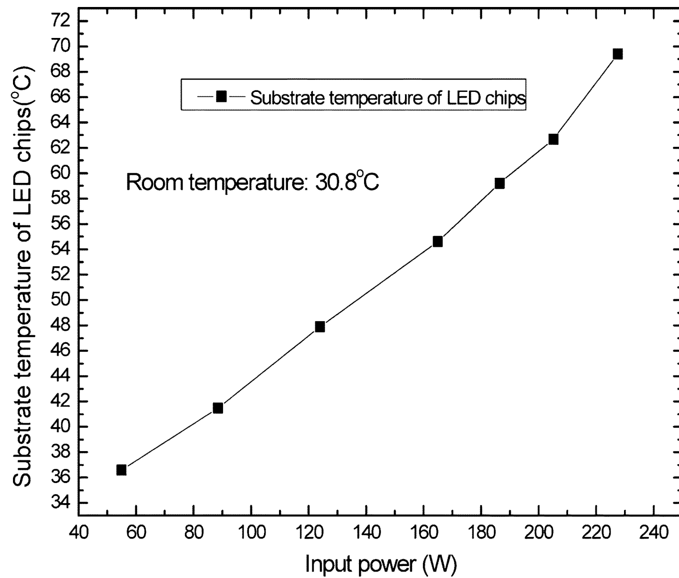


Fig. 16. Variation of LED substrate temperature with input power of a high-power LED lamp.

improves slightly. To make use of the optimization results, refabrication and test for microjet device is proceeded. The optimized microjet array cooling system is used for cooling a 220 W LED lamp; the temperature tests demonstrate it can effectively cool the total system. The substrate temperature of the LED chip in the 227-W LED lamp is just 69.4 °C when the room temperature is about 30.8 °C.

## ACKNOWLEDGMENT

The authors would like to thank Dr. M. Chen, Z. Ma, W. Chen, T. Cheng, and R. Sun for their valuable discussion.

## REFERENCES

[1] A. Zukauskas, M. S. Shur, and R. Gaska*, Introduction to solid-state lighting*. New York: Wiley, 2002, pp. 21–29.

[2] M. Alan, "Solid state lighting-a world of expanding opportunities at LED 2002," *III-Vs Rev.*, vol. 16, no. 1, pp. 30–33, 2003.

[3] N. Narendran and Y. M. Gu, "Life of LED-based white light sources," *IEEE J. Display Technol.*, vol. 1, no. 1, pp. 167–171, Sep. 2005.

[4] M. Arik and S. Weaver, "Chip scale thermal management of high brightness LED packages," in *Proc. SPIE 4th Int. Conf. Solid State Light.*, Denver, CO, 2004, vol. 5530, pp. 214–223.

[5] S. Sano, H. Murata, and K. Hattori, "Development of flat panel LED module with heat sink," *Mitsubishi Cable Ind. Rev.*, vol. 86, pp. 112–118, 1993.

[6] J. Petroski, "Understanding longitudinal fin heat sink orientation sensitivity for Light Emitting Diode (LED) lighting applications," in *Proc. Int. Electron. Packag. Tech. Conf. Exhibition*, Maui, HI, 2003, pp. 111–117.

[7] J. H. Chen, C. K. Liu, Y. L. Chao, and R. M. Tain, "Cooling performance of silicon-based thermoelectric device on high power LED," in *Proc. 24th Int. Conf. Thermoelectrics*, Clemson, SC, 2005, pp. 53–56.

[8] C. C. Hsu, S. J. Wang, and C. Y. Liu, "Metallic wafer and chip bonding for LED packaging," in *Proc. 5th Pacific Rim Conf. Lasers Electro-Optics*, Taipei, Taiwan, 2003, vol. 1, p. 26.

[9] K. Zhang, G. W. Xiao, C. K. Y. Wong, H. W. Gu, M. M. F. Yuen, P. C. H. Chan, and B. Xu, "Study on thermal interface material with carbon nanotubes and carbon black in high-brightness LED packaging with flip-chip," in *Proc. 55th Electron. Compon. Technol.*, Orlando, FL, 2005, pp. 60–65.

[10] T. Acikalin, S. V. Garimella, J. Petroski, and R. Arvind, "Optimal design of miniature piezoelectric fans for cooling light emitting diodes," in *Proc. 9th Intersociety Conf. Thermal Thermomechanical Phenomena Electronic Syst.*, New York, 2004, vol. 1, pp. 663–671.

[11] S. Liu, T. Lin, X. B. Luo, M. X. Chen, and X. P. Jiang, "A microjet array cooling system for thermal management of active radars and high-brightness LEDs," in *Proc. 56th Electronic Compon. Technol. Conf.*, San Diego, CA, 2006, pp. 1634–1638.

[12] S. Wu, J. Mai, Y. C. Tai, and C. M. Ho, "Micro heat exchanger by using MEMS impinging jets," in *Proc. 12th IEEE Int. Conf. Micro Electro Mech. Syst.*, Orlando, FL, 1999, pp. 171–176.

[13] A. S. Fleischer and S. R. Nejad, "Jet impingement cooling of a discretely heated portion of a protruding pedestal with a single round air jet," *Exp. Thermal Fluid Sci.*, vol. 28, pp. 893–901, 2004.

[14] H. Chattopadhyay, "Numerical investigations of heat transfer from impinging annular jet," *Int. J. Heat Mass Transfer*, vol. 47, pp. 3197–3201, 2004.

[15] L. Thielen, H. J. J. Jonker, and K. Hanjali, "Symmetry breaking of flow and heat transfer in multiple impinging jets," *Int. J. Heat Fluid Flow*, vol. 24, pp. 444–453, 2003.

[16] D. H. Lee, J. H. Song, and M. C. Jo, "The effects of nozzle diameter on impinging jet heat transfer and fluid flow," *ASME J. Heat Transfer*, vol. 126, pp. 554–557, 2004.

[17] A. Ramezanpour, H. Shirvani, and I. Mirzaee, "A numerical study on the heat transfer characteristics of two-dimensional inclined impinging jet," in *Proc. 5th Electron. Packag. Technol. Conf.*, Singapore, 2003, pp. 626–632.

**Xiaobing Luo** received the Ph.D. degree from Tsinghua University, Beijing, China, in 2002.

He is an Associate Professor in Huazhong University of Science and Technology (HUST), Wuhan, China. He works at School of Energy and Power Engineering and Wuhan National Laboratory for Optoelectronics in HUST. His main research interests are heat and mass transfer, LED, microfluidics, MEMS, sensors and actuators. He has published more than 30 papers, filed and owned 23 patents in USA, Korea, Japan, Europe, and China.

**Sheng Liu** received the Ph.D. degree from Stanford University, Stanford, CA, in 1992.

He is a specially recruited professor, Director of Institute of Microsystems, Director of MOEMS Division, Wuhan National Laboratory of Optoelectronics, Huazhong University of Science and Technology, Wuhan, China. His main research interests are LED, MEMS, IC packaging, mechanics, sensors. He has published more than 200 technical articles and filed more than 50 patents.